Springer

KSME

Journal of Mechanical Science and Technology 32 (4) (2018) 1793~1804
www.springerlink.com/content/1738-494x(Print)/1976-3824(Online)
DOI 10.1007/s12206-018-0336-0

The effects of ground compliance on flexible planar passive biped dynamic walking †

Yao Wu, Daojin Yao and Xiaohui Xiao*

School of Power and Mechanical Engineering, Wuhan University, Wuhan, 430072, China

(Manuscript Received July 15, 2017; Revised December 7, 2017; Accepted January 17, 2018)

Abstract

Passive biped dynamic walking exhibits humanoid gait. Many efforts have been made to implement a flexible and anthropomorphic passive model. However, the couple of flexible passive walker on compliant ground has not been well studied yet. The objective of this paper was to develop multibody dynamics for flexible passive walker on compliant ground, in which the nonlinear spring-damper contact model was used both in normal and tangential directions to represent ground compliance. Inspired by elastic mechanisms in human locomotion, hip stiffness and damping were incorporated in the proposed flexible passive walker. Different from traditional impact-momentum method, one unified set of continuous dynamics based on continuous force method was developed to describe the entire passive walking gait on compliant ground, including the real double support phase. Through numerical simulations, stable period-one gait and double support phase were gained. After investigating the effects of contact parameters on step length, period and velocity, it was found that larger contact stiffness and smaller contact damping lead to a higher step velocity gait. The adjustment of hip stiffness could be used to improve the versatility of the flexible walker on varying compliant grounds.

Keywords: Biped robot; Compliant ground; Continuous force method; Flexible robot; Passive dynamic walking

1. Introduction

Biped walking is one of the most inspiring and promising locomotion types of robots for its adaptability to work in human environments. Climbing up and down stairs [1], stepping over obstacles [2] and running [3] exhibit the applications and merits of the biped. For many typical biped robots such as the Honda ASIMO [4] and the HRP-4 [5], stable walking could be achieved under "zero moment point" (ZMP) principle [6] by preplanning the trajectory of the biped to make sure the ZMP always remains within the convex hull of the supporting area. Since the ZMP trajectory is usually implemented by high-gain PD controller, the motions achieved by ZMP are conservative, inefficient, and unnatural looking [7]. Another different approach inspired by passive dynamic walking (PDW) has attracted more and more attention to produce humanoid and energy-efficient gaits.

Passive dynamic walking stands for a walking manner where the robot walks down a slope without any actuation [8]. Because the kinetic energy loss of leg-ground impact could be supplemented by gravitational potential energy, passive dynamic walker could move downslope only powered by gravity, exhibiting energy efficient, naturalistic, and highly dynamic gaits. The study of the PDW would be helpful for a better understanding of human locomotion, and provide insights into how to control and develop humanoid robots.

To gain a deeper view to the nonlinear dynamic behaviors of anthropomorphic biped robot, many efforts have been made to design flexible PDW models, such as active leg compliance added in Ref. [9], and ankle compliance used in Ref. [10]. Experiments by Whittington [11] provided quantitative support for the suggestion that passive elastic mechanisms about the hip are utilized during human walking, which implies that elastic energy storage plays an important role in dynamic behavior of biological legged locomotion [12]. Comparisons [13] show that flexible robot where compliant components were added into the model could lead to a more energy-efficient bipedal locomotion. A good design of the flexible model inspired by PDW would be useful to implement an energy-efficient walking gait.

Under appropriate initial conditions, the flexible PDW model could descend a gentle slope ground without active control. The biped robot on the ground is a complex multibody dynamics problem. Most dynamics of PDW were modeled based on the impact-momentum method. The impact-momentum method [14] assumes that the leg-ground impact occupies infinitely short of time, and the configuration of the biped does not change significantly. Based on impact-momentum method, hybrid dynamics were widely used in biped robots modelling [15-17] and gained success to simplify dynamics and be valid in the walking experiments on rigid

*Corresponding author. Tel.: +86 27 6877 2040, Fax.: +86 27 6877 2040
E-mail address: xhxiao@whu.edu.cn
† Recommended by Associate Editor Hak Yi

surface. However, there are two drawbacks of the impact-momentum method in biped robot modelling. First, the duration of double support phase (i.e. two legs contacted with the ground) could not be described since the leg-ground impact is regarded as instantaneous process, which is against the observations that the double support phase does occupy duration in human being's walking cycle [18]. Furthermore, the bipedal walking on compliant ground is beyond the describe of impact-momentum method. Compliant ground is a kind of ground model where elasticity and viscosity of real ground are taken into consideration [19, 20]. In the literature of biped walking, RABBIT gained lower walking speed on compliant surface than the rigid case both in numerical simulations [21] and physical experiments [22]. The reasons were attributed to the increased energy dissipation during impact between robot and compliant ground.

To model bipedal walking on compliant ground, dynamics based on continuous force method could be used. Different from impact-momentum method, continuous force method regards the interaction forces act in a continuous manner during the impact by adding the contact forces to the equations of motions during their action period [14]. Spring-damper equivalent models were built in Refs. [23-25]. Ref. [26] covers the ground reaction forces into the forward dynamic simulations to implement a feedback control system that stabilizes the torso balance for the humanoid robot, while the contact models were built in ADAMS. Hertz contact model in normal direction were used in Ref. [27] and the elastic contact influence on passive walking gait was discussed. LuGre dynamic friction model was used in the tangential direction of passive walker dynamics in Ref. [28], though the authors in Ref. [28] conclude that a friction model with complexity of the LuGre model is not necessary to capture a majority of the dynamic features of the passive gait, since the sliding velocity among two surfaces does remain below the Stribeck velocity. Above analyses put emphasis on the ground compliance, while the flexibility of the robot body is not considered as the robot was modelled as rigid-body. The couple of flexible robot on the compliant ground is not well investigated yet. To the best of the authors' knowledge, there is rare literature discussing the influence of ground compliance on flexible passive dynamic walking.

This paper aims to investigate the effects of ground compliance on flexible passive walker based on continuous force method. The main contributions of this paper lie in modelling flexible passive walker on compliant ground in only *one* unified set of equations and investigating the effects of ground compliance on flexible passive biped walking. Different from widely used compass-like model, one flexible passivity-based biped robot model was proposed. Instead of hybrid dynamics, the multibody dynamics based on continuous force method was built for the flexible biped robot on compliant ground. The effects of ground compliance on the flexible robot were discussed, which would be helpful to guideline design and control of the flexible robot on compliant ground. One advantage of the dynamics this paper presented is that there is no discontinuity at the leg-ground impact moment in the continuous motion equations, which is beneficial to simulate the double support phase of bipedal walking on compliant ground.

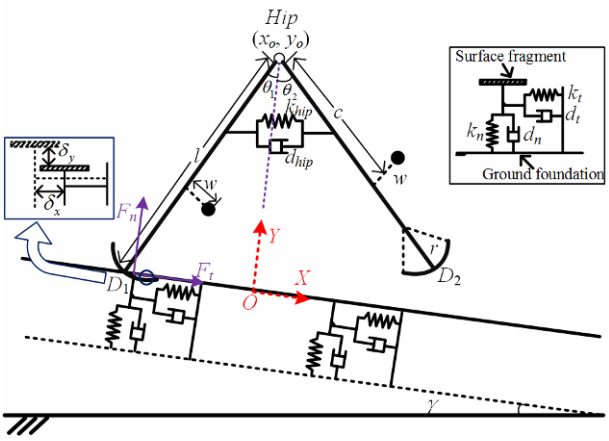

Fig. 1. Model of flexible passive walker.

The rest of the paper is organized as followed: Sec. 2 builds up the multibody dynamics model of the flexible passive biped walker on compliant ground, based on continuous force method. Simulation environment setup and typical passive dynamic walking gait are provided in Sec. 3. Sec. 4 conducts parametric studies of the influence of structural parameter and contact parameters on walking gait. Conclusions are drawn in Sec. 5.

2. Multibody dynamics of robot-ground

In this section, a multibody dynamic model for planar flexible two-link biped passive walker on compliant ground was developed, where compliant ground was modelled as nonlinear spring-damper in normal and tangential direction. Based on continuous force method, there is only *one* set of dynamic equations to describe the entire motion cycle, which is different from widely used hybrid dynamics model.

2.1 Dynamics

This paper considers the planar locomotion, i.e. all motions take place in the sagittal plane. The leg contacting the ground is called the *support leg* and the other is called the *swing leg*. There are two successive phases in one walking period: *Single support phase* means that only one leg contacts the ground, while *double support phase* means two legs touch the ground.

The proposed passive walker model is depicted as Fig. 1. There are some differences between the proposed model with the general compass-like model [29]. First, the arc-shape feet were used in the proposed model, rather than the point feet. To implement a humanoid design, the moment of inertia and mass offset of leg were incorporated in the proposed model. Moreover, spring stiffness k_{hip} and damping d_{hip} inspired by the intrinsic compliance of muscle structure, were added in the hip to imitate the passive mechanisms utilized during human

Table 1. Flexible walker structural parameters.

Parameter	Value
l (m)	0.5
c (m)	0.1
r (m)	0.2
J_l (kg·m^2)	0.0398
w (m)	-0.0025
m_h (kg)	2 kg
m_l (kg)	1 kg
k_{hip} (N·m/rad)	0.95
d_{hip} (N·m·s/rad)	0.018
γ (rad)	0.02
g (kg·m^2)	9.8

being walking.

Specifically, the flexible biped model consists of two identical rigid legs, hinged with frictionless rotary joint (hip). The mass of torso is concentrated as the hip mass m_h. The leg is modelled as a distributed mass, with leg mass m_l, moment of inertia J_l and mass offset w. As shown in the Fig. 1, the length of leg and the distance between hip and the leg mass of center are l and c respectively. The radius of arc-shape feet is r. The flexible biped passive walker is set on a slope at an inclination γ. The parameters of flexible passive biped are shown as Table 1.

The generalized coordinate could be defined as

$$x = [q, \dot{q}] = [x_o, y_o, \theta_1, \theta_2, \dot{x}_o, \dot{y}_o, \dot{\theta}_1, \dot{\theta}_2] \tag{1}$$

where q is the position variable, and $\dot{q}$ is the velocity variable. (x_o, y_o) is the position of hip, $(\dot{x}_o, \dot{y}_o)$ is the velocity of hip. θ_1 is the angular position of the leg with respect to vertical of the rear leg, and θ_2 is the angular position of the leg with respect to vertical of the fore leg. The positive directions of all angles are counter-clockwise. The X axis is set parallel to the slope, with positive direction to the downslope. The Y axis is vertical to the slope, with positive direction to the up. And the coordinate origin lies at hip's projection on the slope [27].

The motion equation based on Lagrange method then becomes

$$M(q)\ddot{q} + C(q, \dot{q})\dot{q} + G(q) = Q_f \tag{2}$$

where $M(q)$ is the inertia matrix, $C(q, \dot{q})$ is the matrix of Coriolis and centrifugal terms, $G(q)$ is the gradient of the potential energy, and Q_f describes the non-conservative forces on the generalized coordinates. More details are provided in Appendix.

Based on continuous force method, the proposed passive dynamic walking model is described by one unified set of Eq. (2) that captures both single support phase and double support phase. The normal contact force F_n and tangential contact force F_t in Q_f were calculated based on non-linear contact models detailed in Secs. 2.2 and 2.3, respectively.

Table 2. Normal contact parameters.

Parameter	Value
k_n (N·m/rad)	1×10^5
d_n (N·m·s/rad)	1×10^6

2.2 Normal contact force

Contact model was used to describe the contact process during the leg-ground impact. Hertz's model [30] is one widely used nonlinear contact model. However, since there is no damping in the Hertz model and its equivalent coefficient of restitution is one, Hertz's model is limited to impacts with elastic deformation, such as low impact speeds and hard materials cases [14].

Hunt-Crossley contact model [31] where hysteretic damping is included, was used in this paper to model the nonlinear contact forces during leg-ground impact. The normal contact force could be described as

$$F_n = k_n \delta_y^{\ m} + d_n \delta_y^{\ p} \dot{\delta}_y^{\ q} \tag{3}$$

where δ_y stands for the interpenetration, and $\dot{\delta}_y$ is the relative interpenetration velocity of the leg-ground. Contact stiffness k_n and damping d_n are constants, depending on material and geometric properties and computed by using elastostatic theory. To be specific, stiffness k_n is defined in terms of Poisson's ratios, Young's moduli and the radii of the two spheres, while damping d_n can be related to the coefficient of restitution. Johnson [30] deduced that m = 1.5 for two spheres in central impact case. And $p = m$ = 1.5, q = 1 is set to the proposed flexible biped dynamics [31]. The normal contact parameters are listed in Table 2.

The normal contact model Eq. (3) could be regarded as a nonlinear spring-damper $F_n = (\delta_y, \dot{\delta}_y)$. The normal imbedded depth δ_y and relative velocity $\dot{\delta}_y$ could be derived from the geometry of flexible biped model. As shown in Fig. 1, there are two points D_1 and D_2 marked on the feet, which is the contact point and impending contact point, respectively. The D_1 and D_2 are the points on the feet with the lowest y coordinate [28]. The deformation and velocity of contact point D_i (i = 1 or 2, corresponds to each foot) in the proposed passive biped model (Fig. 1) were derived as

$$\delta_y = y_{D_i} = y_o - r - (l - r)\cos\theta_i \tag{4}$$

$$\dot{\delta}_y = v_{yD_i} = \dot{y}_o + \dot{\theta}_i(l - r)\sin\theta_i + r\dot{\theta}_i \,. \tag{5}$$

It is noted that normal contact force F_n is only applied on the support leg end. As for the swing leg, since it does not touch the ground, the normal force should be set as zero as

$$\begin{cases} F_{ni} = 0 & \text{if } \delta_{yi} > 0 \\ F_{ni} = k_n \delta_{yi}^m + d_n \delta_{yi}^p \dot{\delta}_{yi}^q & \text{if } \delta_{yi} \le 0 \end{cases} \quad (i = 1, 2) \,. \tag{6}$$

Table 3. Tangential contact parameters.

Parameter	Value
k_t (N·m/rad)	90
d_t (N·m·s/rad)	900
v_s (m/s)	10^{-4}
v_d (m/s)	10^{-3}
μ_s	0.5
μ_d	0.4

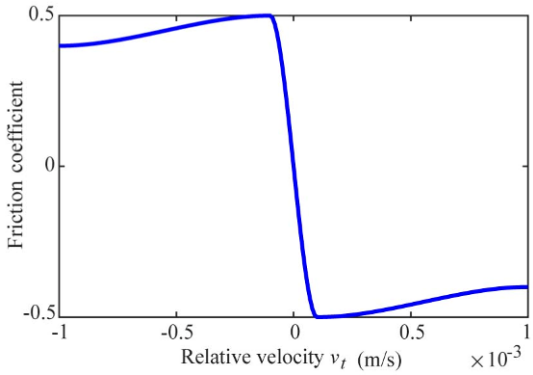

Fig. 2. Coulomb friction coefficient.

2.3 Tangential contact force

The ground compliance would be considered in both normal and tangential directions, though the ground compliance in tangential direction was rarely considered in most previous efforts to model the biped on compliant ground. To describe the viscosity of the ground, a nonlinear spring-damper model in tangential direction was used in this paper. The tangential contact force at the contact point during sticking derived from the Hunt-Crossley model could be described as

$$F_t = k_t \delta_x^m + d_t \delta_x^p \dot{\delta}_x^q \tag{7}$$

where k_t and d_t is the tangential contact stiffness and damping respectively, δ_x and $\dot{\delta}_x$ is the tangential imbedded depth and relative velocity of the contact point D_i respectively, and $p = m = 1.5$, $q = 1$.

As shown in Fig. 1, the tangential deformation and velocity of the contact point D_i could be derived from the geometry as

$$\delta_x = x_{D_i} = x_o + (l-r)\sin\theta_i \tag{8}$$

$$\dot{\delta}_x = v_{xD_i} = \dot{x}_o + r\dot{\theta}_i + \dot{\theta}_i(l-r)\cos\theta_i . \tag{9}$$

In addition, friction should be added into tangential model. The Coulomb friction model was widely used, where there are two possible friction situations: sliding, with $f = \mu_d F_n$; sticking, with $f \le \mu_s F_n$, where μ_d is the coefficient of dynamic friction and μ_s is the coefficient of static friction [14]. A Coulomb friction model [27] was used in this paper as

$$\mu = \begin{cases} \mu_d & v_t \le -v_d \\ \mu_d + (\mu_s - \mu_d)(\dfrac{v_t + v_d}{v_d - v_s})^2 (3 - 2\dfrac{v_t + v_d}{v_d - v_s}) & -v_d \le v_t \le -v_s \\ \mu_s - 2\mu_s (\dfrac{v_t + v_s}{2v_s})^2 (3 - \dfrac{v_t + v_s}{v_s}) & -v_s \le v_t \le v_s \\ -\mu_s + (\mu_s - \mu_d)(\dfrac{v_t - v_s}{v_d - v_s})^2 (3 - 2\dfrac{v_t - v_s}{v_d - v_s}) & v_s \le v_t \le v_d \\ -\mu_d & v_t \ge v_d . \end{cases} \tag{10}$$

The tangential force F_t could be derived as Eq. (11) by combining nonlinear spring-damper contact force and the Coulomb friction. The tangential contact force is only applied on the support leg end. The tangential contact parameters were provided as Table 3, and the Coulomb friction coefficient with respect to relative velocity v_t was depicted as Fig. 2.

$$\begin{cases} F_{ti} = 0 & \text{if } \delta_{xi} > 0 \\ F_{ti} = k_t \delta_{xi}^m + d_t \delta_{xi}^p \dot{\delta}_{xi}^q + \mu F_{ni} & \text{if } \delta_{xi} \le 0 \end{cases} \quad (i = 1,2) . \tag{11}$$

3. Numerical simulation

3.1 Numerical method

Combined the small deformation motions at the contact point D_i and the large rigid body motion of the robot, the dynamics Eq. (2) is one typical *stiff* problem, which could not be solved by ODE45 in MATLAB. Central difference method [32], one *explicit integration method* widely used in hydromechanics [33], was employed in this paper to calculate the stiff dynamics equation. Let Δ_t as the integration step, then the equal step calculation process could be described as [33]:

$$\begin{aligned} (\frac{1}{\Delta_t^2} M + \frac{1}{2\Delta_t} C) \cdot U_{n+1} = Q_f - G + \frac{2}{\Delta_t^2} M \cdot U_n \\ -(\frac{1}{\Delta_t^2} M - \frac{1}{2\Delta_t} C) \cdot U_{n-1} . \end{aligned} \tag{12}$$

At first, initialization process was finished as

$$U_0 = q_0, \dot{U}_0 = \dot{q}_0 \tag{13}$$

$$\ddot{U}_0 = M^{-1} \cdot (Q_f - C \cdot \dot{q}_0 - G) \tag{14}$$

$$U_{-1} = U_0 - \Delta_t \cdot \dot{U}_0 + \Delta_t^2 / 2 \cdot \ddot{U}_0 . \tag{15}$$

Then, the n^{th} iteration step could be described as

$$\begin{aligned} U_{n+1} = (\frac{1}{\Delta_t^2} M + \frac{1}{2\Delta_t} C)^{-1} \Big[Q_f - G + \\ \frac{2}{\Delta_t^2} M \cdot U_n - (\frac{1}{\Delta_t^2} M - \frac{1}{2\Delta_t} C) \cdot U_{n-1} \Big] \end{aligned} \tag{16}$$

$$\dot{U}_{n+1} = \frac{U_{n+1} - U_{n-1}}{2\Delta_t} \tag{17}$$

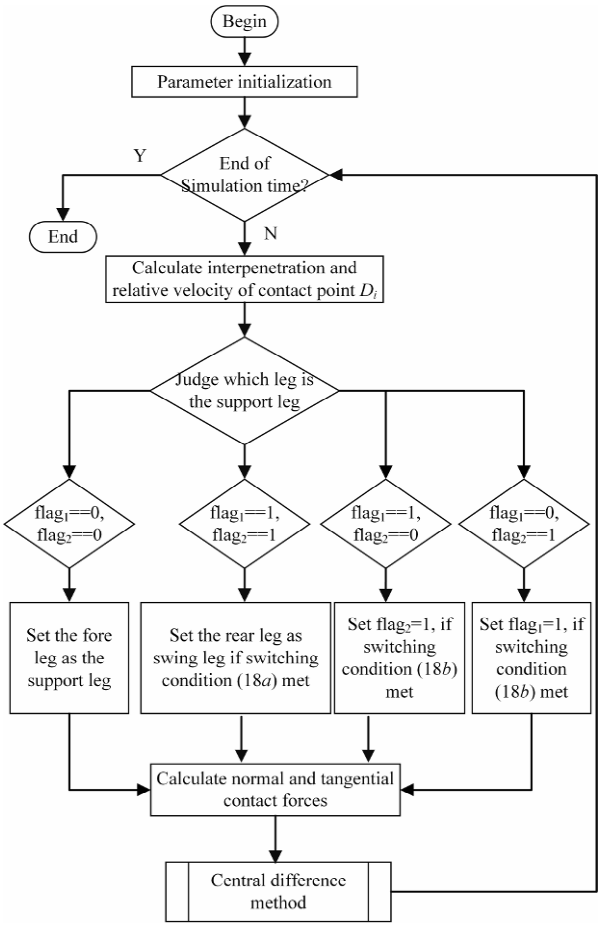

Fig. 3. Flow chart for the stiff dynamics solver.

and the iteration result would be gained as $x_{n+1} = [q_{n+1}, \dot{q}_{n+1}] = [U_{n+1}, \dot{U}_{n+1}]$.

Since only the support leg touches the ground, normal and tangential contact forces are just applied on the support leg end. Two flags were introduced to mark the leg status. The case $flag_i = 0$ ($i = 1,2$) stands for the concerned leg is the swing leg ($F_{ni} = 0$, $F_{ti} = 0$), while $flag_i = 1$ stands for the leg is the support leg. The switching conditions could be described as Eq. (18), to distinguish the forces applied on the leg end.

$$\begin{cases} flag_i = 0 & if \ \delta_i > 0 \ \& \ \dot{\delta}_i > 0 \quad (18a) \\ flag_i = 1 & if \ \delta_i < 0 \ \& \ \dot{\delta}_i < 0 . \quad (18b) \end{cases}$$

The flow chart of stiff dynamics solver based on central difference method is depicted as Fig. 3. Every iteration step, the status of each leg is evaluated, and contact force is only applied on the support leg end. The central difference method equations are listed as Eqs. (13)-(17).

3.2 Typical walking gait

Under proper structural parameters and initial values, the flexible passive biped dynamic walker could move downslope without any actuation. Period-one gait in passive dynamic walking corresponds to the fixed point of dynamic system, which could be derived by the Cell Mapping method [34].

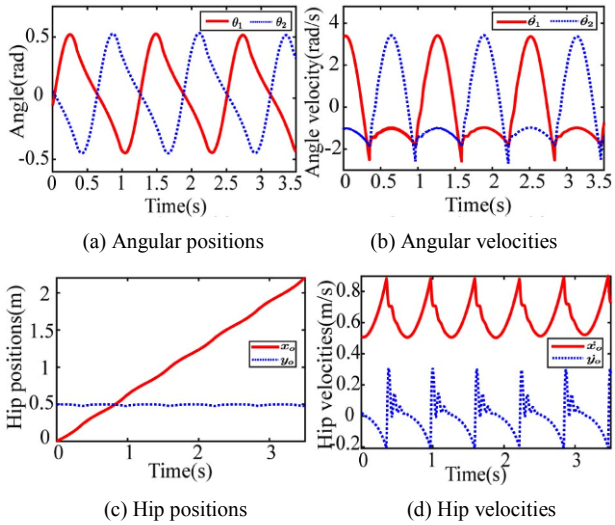

(a) Angular positions (b) Angular velocities

(c) Hip positions (d) Hip velocities

Fig. 4. Period-one gait.

One typical period-one gait was gained under flexible walker structural parameters (Table 1), the normal contact parameters (Table 2), the tangential contact parameter (Table 3), and initial condition x_0 = [0, 0.4969, -0.0582, 0.0582, 0.5092, 0.0186, 3.3338, -1.0093]. The simulated time is 3.5 s, and the integration step is 10^{-4} s.

Fig. 4 shows the simulation results of typical PDW gait. The periodicity of Fig. 4 shows the success of walking gait. Besides, it can be seen from the Figs. 4(b) and (d) that due to the effects of contact forces from compliant ground and the existence of double support phase, there are some fluctuations at the impact duration for the angle velocities (Fig. 4(b)) and hip velocities (Fig. 4(d)), which is different from immediate changes of the hybrid dynamics. Furthermore, both the positions and velocities in Fig. 4 are continuous, and there is no sudden change of robot's joint velocity.

The stick picture of passive walker is delineated as Fig. 5. For simplicity, the arc-shape of feet are not displayed. It is clear from Fig. 5 that flexible passive walker could descend slope successfully. The double support phase only consists small duration in the bipedal locomotion.

The normal and tangential contact forces were depicted as Fig. 6, both continuously over time. From Fig. 6(a), the normal force peaks at the contact instant, and reaches its steady point after some time of fluctuation. The steady value of normal force is almost the gravity force of the passive walker. Tangential force in Fig. 6(b) has a peak value at the contact moment then has a smooth curve, indicating the friction force in the rotating period of the support leg. Furthermore, the friction changes from the negative to positive as the foot moves forward to backward in the rotation process.

A deeper insight to the normal force, real *double support phase* could be found as Fig. 7(a) shows. From 2.214 s to

Table 4. Soft and slippery compliant ground parameters.

Parameter	Value
k_n (N·m/rad)	0.5×10^5
d_n (N·m·s/rad)	0.5×10^6
k_t (N·m/rad)	10
d_t (N·m·s/rad)	200
μ_s	0.3
μ_d	0.2

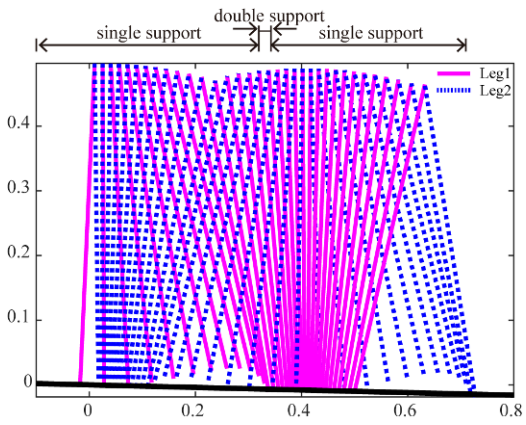

Fig. 5. Stick picture.

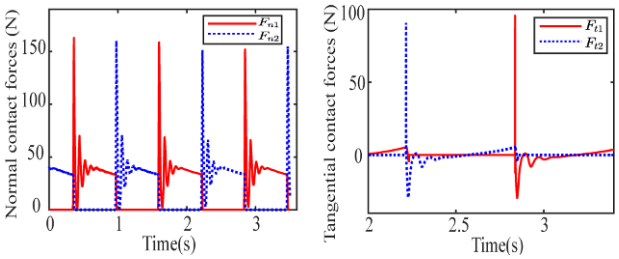

(a) Normal contact forces (b) Tangential contact forces

Fig. 6. Contact forces.

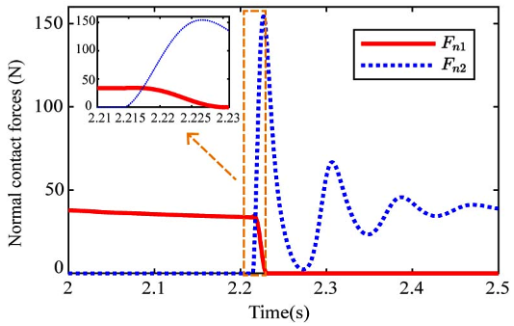

(a) DSP based on contact parameters in Tables 2 and 3

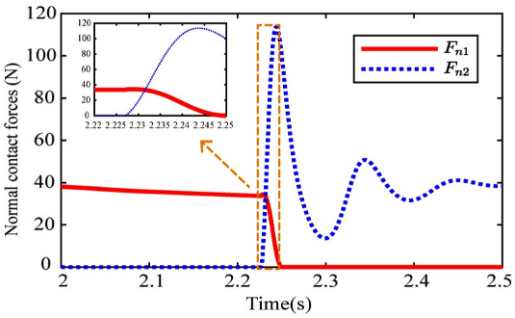

(b) DSP based on contact parameters in Table 4

Fig. 7. Double support phase.

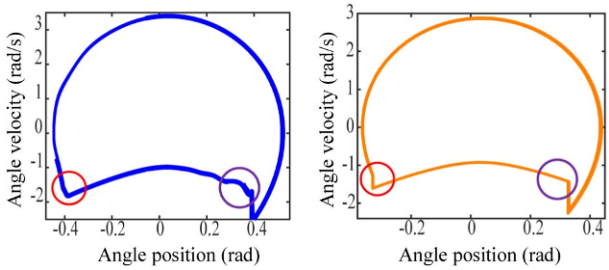

(a) Continuous force method (b) Hybrid dynamics

Fig. 8. Limit cycles under structural parameter in Table 1.

2.231 s, two legs both contacted with the ground at the same time which implies the exist of double support phase. So the double support phase occupies almost 2.71 % in one walking cycle (0.6275 s) in Fig. 7(a). Fig. 7(b) shows that the duration of double support phase would be longer (0.022 s, 3.49 % of period 0.631 s) when flexible passive model walks on soft and slippery compliant ground (contact parameters as Table 4 while keep the other parameter all the same).

One advantage of the dynamics this paper presented based on continuous force method, is that there is no discontinuity at the leg-ground impact, which is useful to simulate the double support phase of flexible biped on compliant ground. Due to the double support phase, the limit cycle shown as Fig. 8(a) would be different from the limit cycle of hybrid dynamics based on impact-momentum method as Fig. 8(b), under the same structural parameters. From Fig. 8, it could be seen that the duration of the double support phase would lead to continuous changes of limit cycle at the switching zone, different from the sudden changes in the hybrid dynamics.

To test the stability of period-one PDW gait, some disturbance was added to the initial value and set x_0 as [0, 0.4840, 0.3285, -0.3285, 0.6875, 0.1375, -1.4206, -1.2684]. Keep other parameters as normal contact parameter Table 2, tangential contact and friction parameter Table 3. Corresponding gait was delineated as Fig. 9. After some adjustment steps, one steady periodic gait could be gained, which implies the stability of the proposed flexible model.

4. Discussions

4.1 Influence of flexible walker structural parameters

To get more details of the dynamics of the PDW and provide a deeper understanding of the human locomotion, the influence of flexible structural parameters on walking gaits

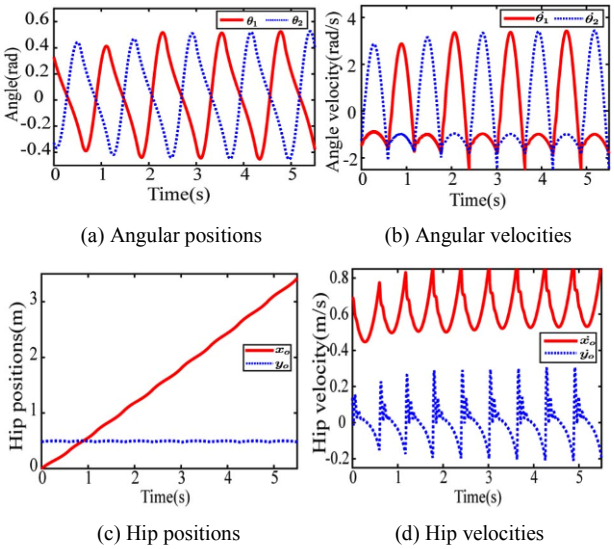

(a) Angular positions (b) Angular velocities

(c) Hip positions (d) Hip velocities

Fig. 9. Gait under disturbed origin value.

was analyzed. To investigate parameters' effects on passive gait, the single variable method (i.e. only one factor is changed from trial to trial [35]) is employed. Three gait descriptors were used in this paper to judge walking gait: Step length L defined as the tangential distance between the position of swing leg end leaves the ground and touches the ground in one walking cycle as Fig. 10, step period P defined as the time from swing leg end leaves the ground till the moment swing leg contacts the ground, and step velocity v defined as L/P.

The main flexible structural parameters of the proposed model include hip mass m_h , leg mass m_l , moment of inertia J_l, mass offset w , and radius of arc-shape feet r. The influence of structural parameters on walking gait was summarized as Table 5. Since the proposed model of this paper covers many flexible robot body parameters, such analysis could be useful to guide better humanoid design for passive walking prototype.

4.2 Influence of normal ground compliance

The contact parameters (i.e. contact stiffness k and damping d) in nonlinear spring-damper model are important to calculate the contact forces. Analytic solution based on contact mechanics [30] is limited to strict physical geometrical assumptions. Experiments are needed to determine the coefficient values, such as Ref. [28] validates the Hunt-Crossley contact model based on a physical passive walker. However, experiments call for high precise equipment and are time-consuming. The normal contact parameters in Table 2 are inspired by Ref. [27].

In the normal direction, normal contact parameters consist of contact stiffness k_n and damping d_n. The contact stiffness k_n stands for the *rigidity* of the foot and the ground. Let contact stiffness k_n vary from 0.5×10^5 to 2.5×10^5. To investigate the flexible passive walker's adjustability to ground compliance, let hip stiffness k_{hip} vary from 0.9 to 1, while other parameters

Table 5. Effects of structural parameters.

Parameter	Step length	Step period	Step velocity
m_h ↑	↑	Invariant	↑
J_l ↑	↑	↑	↓
c ↑	↓	↑	↓
w ↑	↑	↓	↑
r ↑	↑	↓	↑

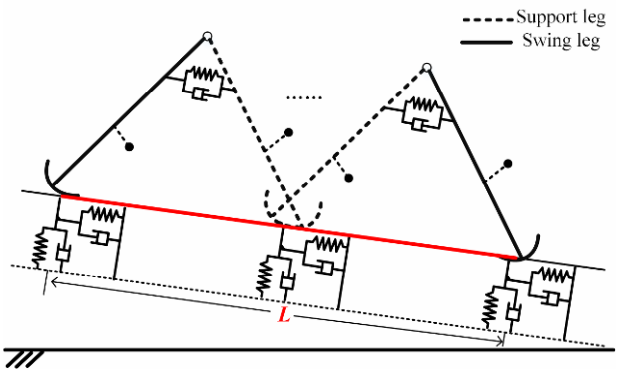

Fig. 10. Step length.

keeps the same as Sec. 3. Every time only one parameter in dynamics changes. Fig. 11 shows the step length, period, and step velocity of the passive dynamic walking on compliant ground respectively.

For the fixed hip stiffness, e.g. k_{hip} = 0.95, though periodic passive walking could still be gained as the increase of normal contact stiffness from 0.5×10^5 to 2.5×10^5, the step length generally increases from 0.3967 m to 0.3976 m (Fig. 11(a)), the step period decreases from 0.622 s to 0.620 s (Fig. 11(b)), and the step velocity increases from 0.6375 m/s to 0.641 m/s (Fig. 11(c)). The step length and velocity rise with increasing normal contact stiffness, which implies that a slower walking gait would be gained on a soft ground. As for the fixed normal contact stiffness, the increase of hip stiffness would lead to the decrease of step length and walking period, but the increased walking velocity. So the energy stored in the hip would help to increase the walking velocity and the change of hip stiffness would be used to control walking velocity on different compliant grounds.

Fig. 12 shows the influence of normal contact damping on passive gait. For the fixed hip stiffness, e.g. k_{hip} = 0.95, as the increase of the normal damping from 0.5×10^6 to 2.5×10^6, the step length decreases from 0.405 m to 0.389 m, the period decreases from 0.625 s to 0.617 s, and the walking velocity decreases from 0.648 m/s to 0.631 m/s, which implies that the lower velocity achieved for more energy dissipated. A faster passive walking gait could be gained on small contact damping ground. As for the fixed normal contact damping, the increase of the hip stiffness would lead to the decrease of step length and the walking period, while the increased walking

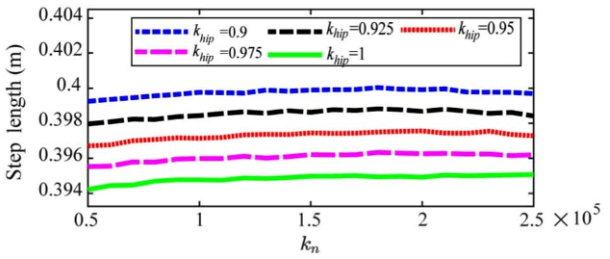

(a) Step length

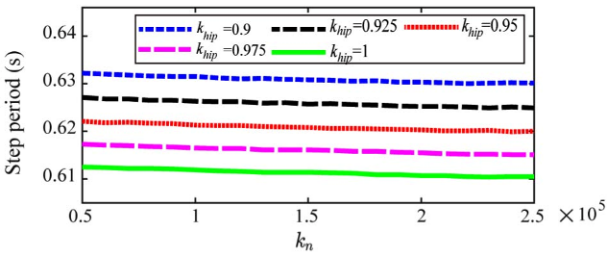

(b) Step period

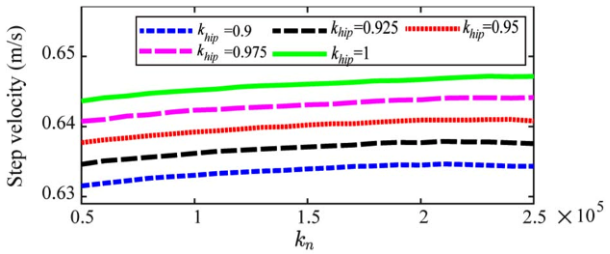

(c) Step velocity

Fig. 11. Influence of normal contact stiffness.

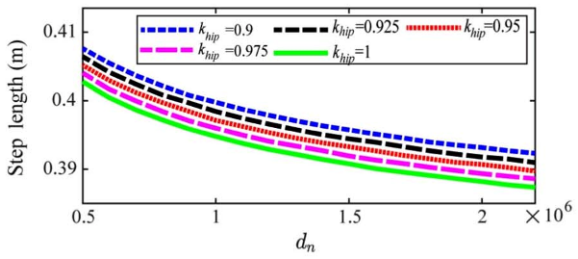

(a) Step length

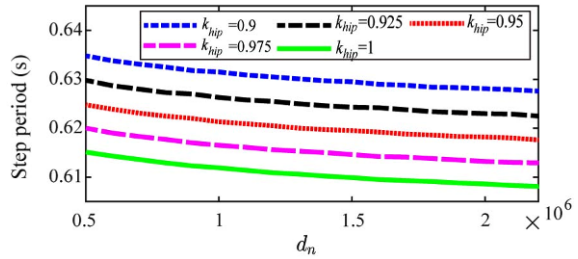

(b) Step period

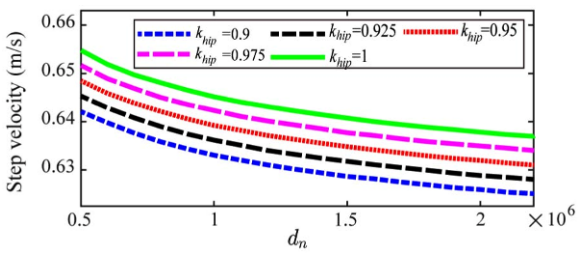

(c) Step velocity

Fig. 12. Influence of normal contact damping.

velocity. So the flexible components incorporated in the proposed model enhance the adaptability of flexible passive walker on compliant ground.

4.3 Influence of tangential contact compliance

Tangential contact compliance could be used to describe the viscosity of the ground. Let the tangential contact stiffness k_t vary from 10 to 85, while other parameters keep the same as Sec. 3. And let hip stiffness vary from 0.9 to 1 for every iteration. It can be seen from Fig. 13 that as k_{hip} = 0.95, the step length increases from 0.39 m to 0.464 m, the step period decreases from 0.626 s to 0.611 s, and the step velocity increases from 0.62 m/s to 0.76 m/s. So a faster passive walking could be achieved on ground with larger tangential contact stiffness. For the fixed normal contact stiffness, the increase of hip stiffness would lead to the decrease of step length and the walking period, while the increased walking velocity. Though the hip elastic mechanism may have minor influence on step velocity, flexible passive walker still gained successful walking over different sticky compliant grounds.

With respect to tangential contact damping d_t, results are depicted in Fig. 14. Let k_{hip} = 0.95, and it could be seen that with the increase of d_t from 100 to 1000, the step length decreases from 0.42 m to 0.393 m, the walking period increases from 0.603 s to 0.623 s, and the gait velocity decreases from 0.696 m/s to 0.63 m/s. Results also showed with that more energy dissipated in tangential direction, lower walking speed gained. Furthermore, though the increase of hip stiffness leads to the higher step velocity, the change amplitude of step velocity is within a small scope.

5. Conclusion and future work

In this paper, a numerical study was performed to investigate the effects of the ground compliance on planar flexible biped passive dynamic walker. Based on continuous force method, one unified set of dynamics equations for the flexible passive walker on compliant ground was built, capturing the entire passive dynamic gait including both the single support phase and double support phase. The central difference method was used to solve the stiff nonlinear dynamics. The influence of the ground compliance was investigated.

We can conclude as follows: (1) One flexible passive biped walker model with arced feet, hip torsional spring stiffness and damping was proposed, to implement an anthropomorphic biped model. (2) One set of dynamics based on continuous force method was built, while the compliant ground was mod-

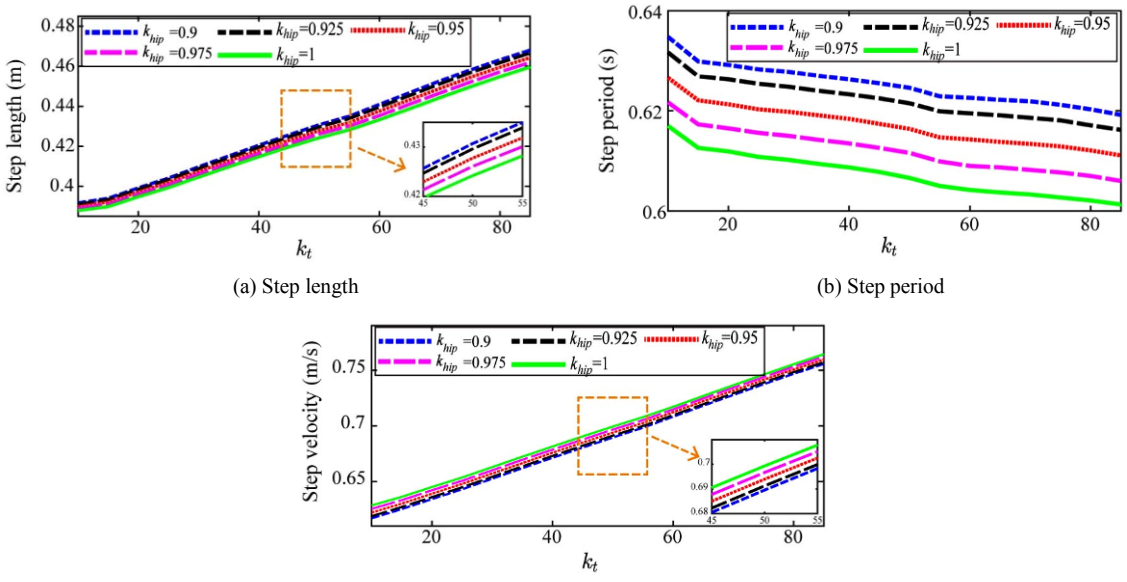

(a) Step length (b) Step period

(c) Step velocity

Fig. 13. Influence of tangential contact stiffness.

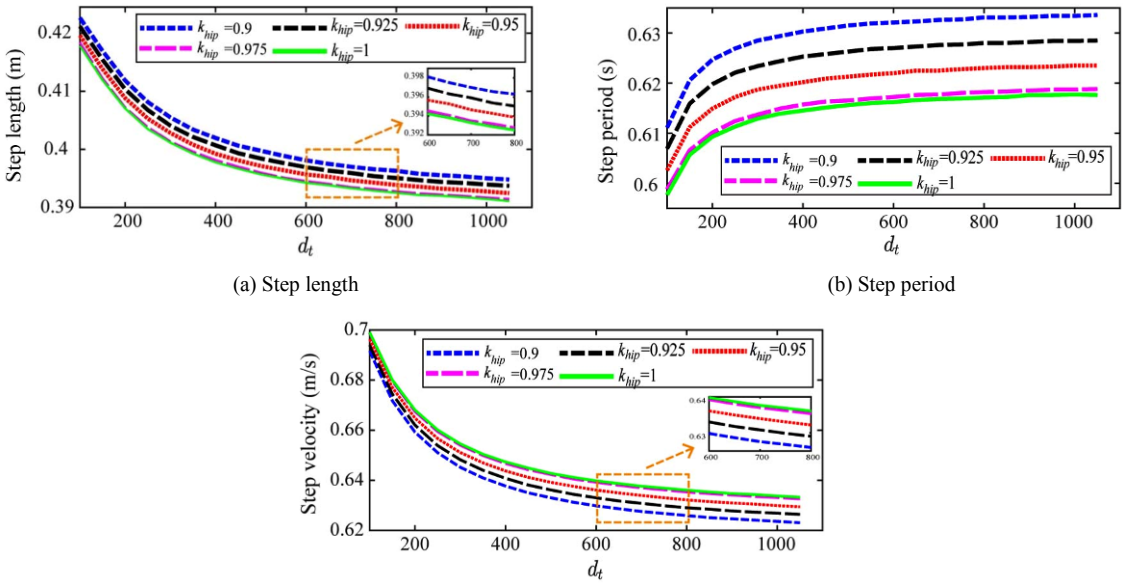

(a) Step length (b) Step period

(c) Step velocity

Fig. 14. Influence of tangential contact damping.

elled as nonlinear spring-damper both in normal and tangential directions. Typical PDW gait was simulated with the aid of central difference method and the double support phase could be evaluated by the dynamics this paper proposed. (3) An elaborate investigation of the effects of the ground compliance on flexible walker was conducted. Results show the increase of contact stiffness both in normal and tangential directions leads to the increase of walking velocity, while the increase of contact damping results in the decrease of walking velocity, which implies slower walking would be gained under soft and sticky grounds. Besides, the passive hip mechanisms in the flexible biped model could be used to improve the adaptability of the model on different compliant grounds.

In the future work, the control approach of adjusting the hip stiffness and damping to implement stable walking on varying compliant grounds will be studied. And the physical flexible walker will be built to validate the model of this paper.

Acknowledgement

This research was supported by National Natural Science Foundation of China (NSFC, Grant No. 51675385 and

51175383). Part of numerical calculations in this paper have been done on the supercomputing system in the Supercomputing Center of Wuhan University.

Nomenclature

l	: Length of leg
c	: Leg distance between hip and the mass center of leg
r	: Radius of arc-shape feet
J_l	: Moments of inertia to the mass center of leg
w	: Mass offset of leg
m_h	: Mass of hip
m_l	: Mass of leg
k_{hip}	: Torsional spring stiffness of hip
d_{hip}	: Damping of hip
γ	: Slope angle
g	: Gravitational acceleration
k_n	: Normal contact stiffness of the ground
d_n	: Normal contact damping of the ground
k_t	: Tangential contact stiffness of the ground
d_t	: Tangential contact damping of the ground
v_s	: Viscous velocity
v_d	: Stiction velocity
μ_s	: Static friction coefficient
μ_d	: Dynamic friction coefficient

References

[1] O. Kwon, K. S. Jeon and J. H. Park, Optimal trajectory generation for biped robots walking up-and-down stairs, *Journal of Mechanical Science and Technology*, 20 (5) (2006) 612-620.

[2] Z. Xia, J. Xiong and K. Chen, Global navigation for humanoid robots using sampling-based footstep planners, *IEEE/ASME Transactions on Mechatronics*, 16 (4) (2011) 716-723.

[3] K. Sreenath, H. W. Park and J. W. Grizzle, Design and experimental implementation of a compliant hybrid zero dynamics controller with active force control for running on MABEL, *2012 IEEE International Conference on Robotics and Automation (ICRA),* Saint Paul, MN, USA (2012) 51-56.

[4] Y. Sakagami, R. Watanabe, C. Aoyama, S. Matsunaga, N. Higaki and K. Fujimura, The intelligent ASIMO: System overview and integration, *2002 IEEE/RSJ International Conference on Intelligent Robots and Systems*, Lausanne, Switzerland (2002) 2478-2483.

[5] K. Kaneko, F. Kanehiro, M. Morisawa, K. Akachi, G. Miyamori, A. Hayashi and N. Kanehira, Humanoid robot HRP-4 - humanoid robotics platform with lightweight and slim body, *2011 IEEE/RSJ International Conference on Intelligent Robots and Systems (IROS)*, San Francisco, CA, USA (2011) 4400-4407.

[6] M. Vukobratović and J. Stepanenko, On the stability of anthropomorphic systems, *Mathematical Biosciences*, 15 (1-2) (1972) 1-37.

[7] I. R. Manchester, U. Mettin, F. Iida and R. Tedrake, Stable dynamic walking over uneven terrain, *The International Journal of Robotics Research,* 30 (3) (2011) 265-279.

[8] T. McGeer, Passive dynamic walking, *The International Journal of Robotics Research,* 9 (2) (1990) 62-82.

[9] R. Q. Van Der Linde, Active leg compliance for passive walking, *Proceedings of 1998 IEEE International Conference on Robotics and Automation*, Leuven, Belgium (1998) 2339-2344.

[10] Q. Wang, Y. Huang and L. Wang, Passive dynamic walking with flat feet and ankle compliance, *Robotica*, 28 (3) (2010) 413-425.

[11] B. Whittington, A. Silder, B. Heiderscheit and D. G. Thelen, The contribution of passive-elastic mechanisms to lower extremity joint kinetics during human walking, *Gait & Posture*, 27 (4) (2008) 628-634.

[12] Y. Or and M. Moravia, Analysis of foot slippage effects on an actuated spring-mass model of dynamic legged locomotion, *International Journal of Advanced Robotic Systems*, 13 (2) (2016) 69.

[13] T. Narukawa, M. Takahashi and K. Yoshida, Efficient walking with optimization for a planar biped walker with a torso by hip actuators and springs, *Robotica*, 29 (4) (2011) 641-648.

[14] G. Gilardi and I. Sharf, Literature survey of contact dynamics modelling, *Mechanism and Machine Theory*, 37 (10) (2002) 1213-1239.

[15] J. W. Grizzle, G. Abba and F. Plestan, Asymptotically stable walking for biped robots: Analysis via systems with impulse effects, *IEEE Transactions on Automatic Control*, 46 (1) (2001) 51-64.

[16] J. W. Grizzle, C. Chevallereau, R. W. Sinnet and A. D. Ames, Models, feedback control, and open problems of 3D bipedal robotic walking, *Automatica,* 50 (8) (2014) 1955-1988.

[17] K. An, Z. Fang, Y. Li and Q. Chen, Internal features in basin of attraction of the simplest walking model, *Journal of Mechanical Science and Technology*, 29 (11) (2015) 4913-4921.

[18] M. W. Whittle, *Gait analysis, An introduction*, Butterworth-Heinemann, Oxford, UK (1991).

[19] I. Takewaki, Probabilistic critical excitation for MDOF elastic-plastic structures on compliant ground, *Earthquake Engineering & Structural Dynamics*, 30 (9) (2001) 1345-1360.

[20] K. Kojima and I. Takewaki, Closed-form critical earthquake response of elastic-plastic structures on compliant ground under near-fault ground motions, *Frontiers in Built Environment*, 2 (2016) 1.

[21] F. Plestan, J. W. Grizzle, E. R. Westervelt and G. Abba, Stable walking of a 7-DOF biped robot, *IEEE Transactions on Robotics and Automation,* 19 (4) (2003) 653-668.

[22] E. R. Westervelt, J. W. Grizzle, C. Chevallereau, J. H. Choi and B. Morris, *Feedback control of dynamic bipedal robot locomotion*, CRC Press, USA (2007).

[23] P. S. Freeman and D. E. Orin, Efficient dynamic simulation of a quadruped using a decoupled tree-structure approach, *The International Journal of Robotics Research,* 10 (6) (1991) 619-627.
[24] D. W. Marhefka and D. E. Orin, Simulation of contact using a nonlinear damping model, *Proceedings of 1996 IEEE International Conference on Robotics and Automation,* Minneapolis, MN, USA (1996) 1662-1668.
[25] Y. Wang, J. Ding and X. Xiao, An adaptive feedforward control method for under-actuated bipedal walking on the compliant ground, *International Journal of Robotics and Automation*, 32 (1) (2017) 63-77.
[26] M. Peasgood, E. Kubica and J. McPhee, Stabilization of a dynamic walking gait simulation, *Journal of Computational and Nonlinear Dynamics*, 2 (1) (2007) 65-72.
[27] F. Qi, T. Wang and J. Li, The elastic contact influences on passive walking gaits, *Robotica*, 29 (5) (2011) 787-796.
[28] D. Koop and C. Q. Wu, Passive dynamic biped walking-Part I: Development and validation of an advanced model, *Journal of Computational and Nonlinear Dynamics*, 8 (4) (2013) 041007.
[29] A. Goswami, B. Thuilot and B. Espiau, A study of the passive gait of a compass-like biped robot: Symmetry and chaos, *The International Journal of Robotics Research*, 17 (12) (1998) 1282-1301.
[30] K. L. Johnson, *Contact mechanics*, Cambridge University Press (1987).
[31] K. H. Hunt and F. R. E. Crossley, Coefficient of restitution interpreted as damping in vibroimpact, *Journal of Applied Mechanics*, 42 (2) (1975) 440-445.
[32] K. J. Bathe, *Finite element procedures in engineering analysis*, Prentice-Hall, New Jersey, USA (1982).
[33] P. Eberhard and B. Hu, *Advanced contact dynamics*, Southeast University Press, Nan-Jing, China (2003).
[34] C. S. Hsu, *Cell to cell mapping: A method of global analysis for nonlinear systems*, Springer Science+Business Media, New York, USA (1987).
[35] D. D. Frey and H. Wang, Adaptive one-factor-at-a-time experimentation and expected value of improvement, *Technometrics*, 48 (3) (2006) 418-431.

Appendix

The dynamic model could be described as

$$\frac{d}{dt}\left(\frac{\partial L(q,\dot{q})}{\partial \dot{q}}\right)-\frac{\partial L(q,\dot{q})}{\partial q}=Q_f \tag{A.1}$$

where the Lagrange function $L=K(q,\dot{q})-V(q)$ and $K(q,\dot{q})=\frac{1}{2}\dot{q}^T D(q)\dot{q}$, $V(q)$ is the kinematic and potential energy, respectively.

$$M(q)\ddot{q}+C(q,\dot{q})\dot{q}+G(q)=Q_f \tag{A.2}$$

where $M(q)$ is the inertia matrix, $C(q,\dot{q})$ is the matrix of Coriolis and centrifugal terms, $G(q)=\frac{\partial V}{\partial q}$ is the gradient of the potential energy, and Q_f describes the nonconservative forces on the generalized coordinates.

$$M(q)=\begin{bmatrix} M_{11} & M_{12} & M_{13} & M_{14} \\ M_{21} & M_{22} & M_{23} & M_{24} \\ M_{31} & M_{32} & M_{33} & M_{34} \\ M_{41} & M_{42} & M_{43} & M_{44} \end{bmatrix} \tag{A.3}$$

where $M_{11}=m_h+2m_l$, $M_{12}=0$, $M_{13}=m_l(c\cdot\cos\theta_1-w\cdot\sin\theta_1)$, $M_{14}=m_l\cdot(c\cdot\cos\theta_2-w\cdot\sin\theta_2)$, $M_{21}=M_{12}$, $M_{22}=m_h+2\cdot m_l$, $M_{23}=m_l\cdot(c\cdot\sin\theta_1+w\cdot\cos\theta_1)$, $M_{24}=m_l\cdot(c\cdot\sin\theta_2+w\cdot\cos\theta_2)$, $M_{31}=M_{13}$, $M_{32}=M_{23}$, $M_{33}=m_l\cdot c^2+m_l\cdot w^2+J_l$, $M_{34}=0$, $M_{41}=M_{14}$, $M_{42}=M_{24}$, $M_{43}=M_{34}$, $M_{44}=m_l\cdot c^2+m_l\cdot w^2+J_l$

$$C(q,\dot{q})=\begin{bmatrix} 0 & 0 & -\dot{\theta}_1 m_l(c\cdot\sin\theta_1+w\cdot\cos\theta_1) & -\dot{\theta}_2 m_l(c\cdot\sin\theta_2+w\cdot\cos\theta_2) \\ 0 & 0 & \dot{\theta}_1 m_l(c\cdot\cos\theta_1-w\cdot\sin\theta_1) & \dot{\theta}_2 m_l(c\cdot\cos\theta_2-w\cdot\sin\theta_2) \\ 0 & 0 & 0 & 0 \\ 0 & 0 & 0 & 0 \end{bmatrix}$$

$$G(q)=\begin{bmatrix} -g\sin\gamma\cdot(m_h+2m_l) \\ g\cos\gamma\cdot(m_h+2m_l) \\ k_{hip}(\theta_1-\theta_2)-cgm_l\sin(\gamma-\theta_1)+gm_l w\cos(\gamma-\theta_1) \\ k_{hip}(\theta_2-\theta_1)-cgm_l\sin(\gamma-\theta_2)+gm_l w\cos(\gamma-\theta_2) \end{bmatrix}$$

$$Q_f=\begin{bmatrix} F_{t1}+F_{t2} \\ F_{n1}+F_{n2} \\ F_{n1}(l-r)\sin\theta_1+F_{t1}((l-r)\cos\theta_1+r)-d_{hip}(\dot{\theta}_1-\dot{\theta}_2) \\ F_{n2}(l-r)\sin\theta_2+F_{t2}((l-r)\cos\theta_2+r)+d_{hip}(\dot{\theta}_1-\dot{\theta}_2) \end{bmatrix}.$$

This model in state space could be described as

$$\dot{x}=\begin{bmatrix} \dot{q} \\ M^{-1}(q)[Q_f-C(q,\dot{q})\dot{q}-G(q)] \end{bmatrix}:=f(x). \tag{A.4}$$

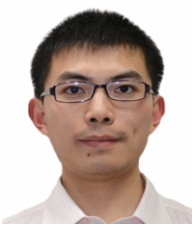

Yao Wu obtained his B.S. in Communication Engineering from Beijing Information Science and Technology University, Beijing, in 2012. Obtained his M.S. in Machine Manufacture and Automation from Beijing Technology and Business University, Beijing, in 2015. Currently, he is pursuing the Ph.D. degree in Mechanical Engineering from Wuhan University, Wuhan, China. His research interests include biped robot dynamics and control.

Daojin Yao obtained his B.S. in Mechanical and Electronic Engineering from East China Jiaotong University, Nanchang, in 2012. He obtained his M.S. in Mechanical and Electronic Engineering from Wuhan University of Technology, Wuhan, in 2015. Currently, he is pursuing a Ph.D. in Mechanical Engineering from Wuhan University, Wuhan, China. His research interests include robot control, electronic circuit design, and embedded programming.

Xiaohui Xiao received the B.S. and M.S. degrees in Mechanical Engineering from Wuhan University, Wuhan, China, in 1991 and 1998, respectively, and the Ph.D. degree in mechanical engineering from Huazhong University of Science and Technology, Wuhan, China, in 2005. She joined the Wuhan University, Wuhan, China, in 1998, where she is currently a Full Professor with the Mechanical Engineering Department, School of Power and Mechanical Engineering. She has published over 30 papers in the areas of mobile robots, dynamics and control, sensors and signal procession. Her current research interests include mobile robotics, high-precision positioning control, and signal processing.